Supplemental Information: Detection of sub-micron thermomechanical and thermochemical failure mechanisms in titanium with a laser-based thermoreflectance technique

Kathleen Quiambao-Tomko[1], Richard R. White[1,2], John A. Tomko[1], Christina M. Rost[3], Lavina Backman[1], Elizabeth J. Opila[1], Patrick E. Hopkins[1,3,4,*]

[1]Department of Materials Science and Engineering, University of Virginia, Charlottesville, Virginia 22904, USA
[2]Nanoscale Materials Characterization Facility, Department of Materials Science and Engineering, University of Virginia, Charlottesville, Virginia 22904, USA
[3]Department of Mechanical and Aerospace Engineering, University of Virginia, Charlottesville, Virginia 22904, USA
[4]Department of Physics, University of Virginia, Charlottesville, Virginia 22904, USA
*email: phopkins@virginia.edu

A: Determination of Incident and Absorbed Power Density

A bulk crystalline SiO_2 substrate with an evaporated 80 nm-thick aluminum surface film was used as the calibration sample for the laser system, in order to measure the applied laser power at the sample and the magnitude of each power step as a function of the laser power output. The thermal properties of the calibration sample were measured using TDTR and are listed in Table S1.

The incident pump and probe powers were measured using a power meter (Newport Laser Power Meter Model: 843-R), which was placed in the laser path immediately preceding the objective lens. The measured power was recorded as a fraction of the laser output power, then fractioned further considering a 10% loss through the objective (measured) and a 7% loss through the quartz chamber window (manufacturer specification). Similarly, the power meter was placed on the sample-chamber side of the dichroic mirror in order to measure the magnitude of the back-aligned pump and probe beams. These power values were measured as a function of laser output power, which was incrementally increased and recorded after each step.

Next, the pump and probe beams were aligned collinearly to the sample and the pump beam was back-aligned to the photodetector. The sample was subjected to the same applied powers as those measured previously using the power meter. The rms voltage outputs from the reflected probe were measured using the lock-in amplifier, again recording the magnitude after each power step increase. We note that the probe-averaged thermal response induced by the pump beam is given by,

$$T_{PA}(t) = \frac{A_0}{4\pi} \int_0^\infty \left(P_t(k,t) + P_0(k,t)\right) \exp\left(-\frac{k^2\left(r_{pump}^2 + r_{probe}^2\right)}{8}\right) k \, dk,$$

and thus independent of the *ratio* of beam sizes.[1]

Table S1: Thermal properties of a Al-SiO₂ calibration sample measured with TDTR and literature values of reflectance coefficients of Al [2] and SiO₂ [3] at the pump and probe wavelengths

Material	Thickness	Thermal Conductivity (W m⁻¹ K⁻¹)	Volumetric Heat Capacity (J K⁻¹ m³)	Reflectance Coefficient
Al	80 nm	150	2.43×10^{-6}	0.87 @ 785 nm 0.94 @ 532 nm
SiO₂	bulk	1.49	1.63×10^{-6}	0.034 @ 785 nm 0.035 @ 532 nm

Using the known parameters for the calibration sample and the proportional relationship between the thermoreflectance signal rise and the applied power based on the radial heat equation (Eq. 1), the absorbed power densities were evaluated using Eq. 2, a linear regression which describes the absorbed power density as a function of the measured power values. The resultant decrease in

power density is due to both the power loss along the path of the laser system and the thermoreflectance properties of the material, e.g., the loss passing through the optical elements, scattering, and the reflected portion of the incident beam at the sample. The reflectance coefficient is taken as constant for each of the pump and probe laser wavelengths and at low applied power densities within the linear regime of the thermoreflectance increase curve (Fig. 2, main manuscript). Thus, the fractional decreases in the calibration sample power densities were applied to power density measurements of the experimental samples in order to normalize the loss from the laser output due to the experimental setup. Likewise, the rms measurements of the probe response to heating were used to obtain the proportionality constant in order to evaluate the absorbance of each material. This method was used to relate the thermoreflectance as a function of increasing power density to the absorbed power, which was subsequently used to approximate the temperature rise both spatially and at critical power densities.

B: Power Density at Failure of Au

In order to demonstrate the influence of both structural and thermally-induced effects on thermoreflectance, a bulk gold (Au) sample was laser irradiated using similar experimental procedures as the Ti metal samples tested in this study. The noble, non-oxidizing properties of Au provide a means to obtain a signal without the effects of a thermally-oxidizing surface, therefore decoupling the response due to temperature rise from the change in reflectance due to this form of microstructural evolution.

Thermoreflectance measurements were conducted in the test chamber under ultrahigh purity Ar gas as described in the main text and recorded as step-wise power sweeps. The signal profiles were obtained as a function of power density through a 10x objective lens with a 4-μm beam radius incident on the Au surface.
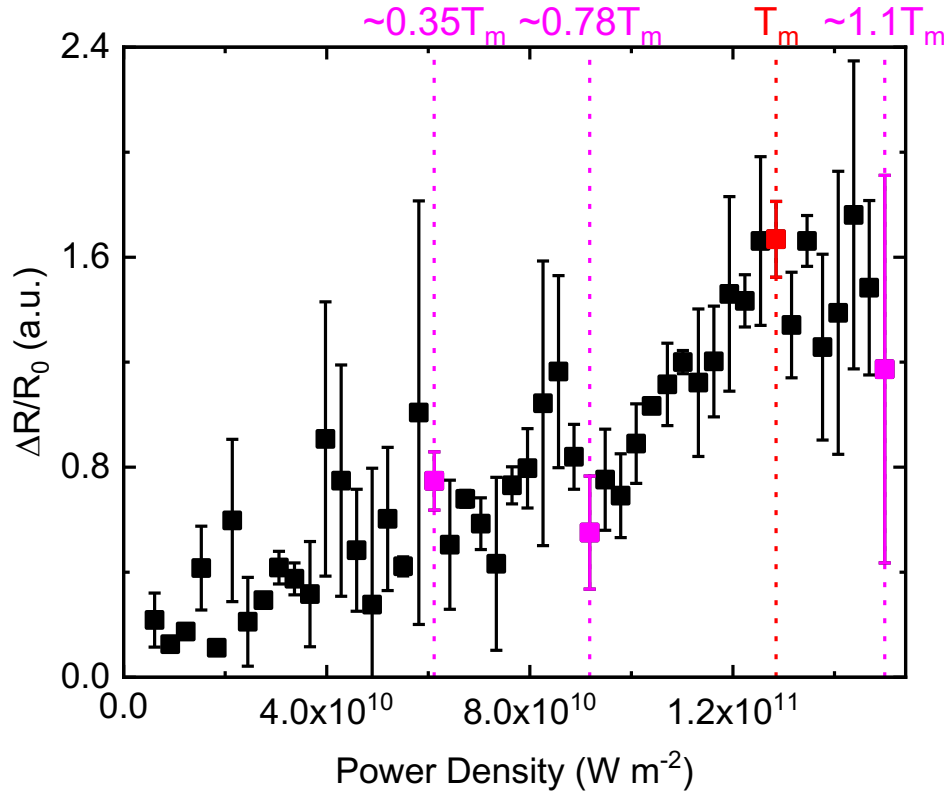

Figure S1. Representative thermoreflectance signal rise profile during a power density sweep of bulk Au monitored until failure. The vertical dashed lines indicate the critical power densities (as described in the main text in Section II) and corresponding temperature rises in the Au that those power density induce (labeled as fraction of gold melting temperature, T_m). The critical points at ~0.35 T_m and ~0.78 T_m indicate morphological changes in bulk Au.[4] The power density at failure roughly correlates to the melting temperature, indicating diffusive heat transfer as the primary failure mode leading to the catastrophic failure event in bulk Au.

The average signal profile for the Au sample is shown in Fig. S1. The critical power densities are denoted with dashed lines and labeled on the top x-axis with their approximate surface temperatures relative to the melting temperature of Au, which were calculated as the steady-state temperature rise at each critical point. Non-linear changes in signal magnitude indicate that the thermoreflectance response deviates from its linear proportionality to temperature rise, as observed previously in the irradiated Ti samples. The approximate temperature rises at these critical points are assumed to be due to incomplete melting of the sample surface, noted to occur in bulk Au metal.[4] Beyond the second critical point, the linear change in thermoreflectance until ultimate signal loss around 1.1 T_m indicates failure due to diffusive heat transfer, i.e., melting.

C: Critical point analysis

An example of our critical point analysis, of which we take the first derivative of the signal and find local minima/maxima to define regions of which the sample is responding in a non-linear fashion, is shown below. Figure S2 contains the data of the first derivative of Fig. 1 in the main text, Fig. S3 contains the first derivative of Ti-18 of Fig. 2a in the main text,
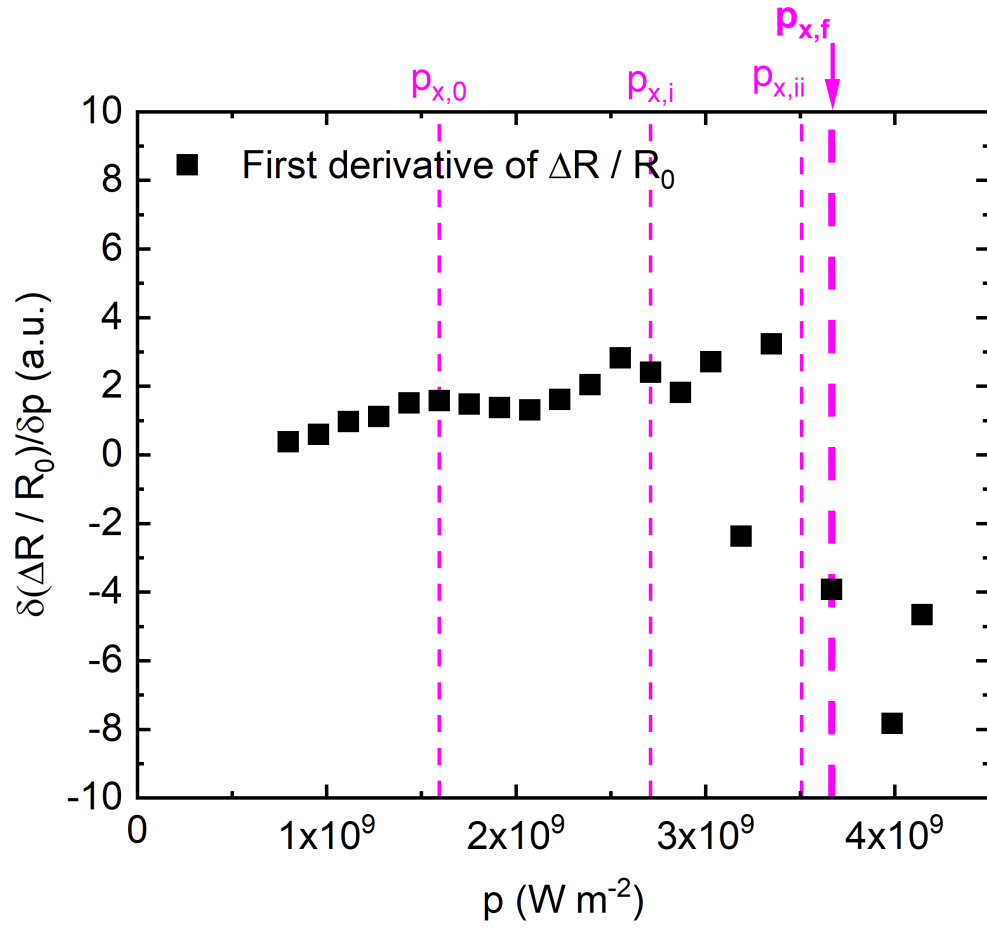
Figure S2. First derivative of our thermoreflectance data shown in Fig. 1 in the main manuscript.
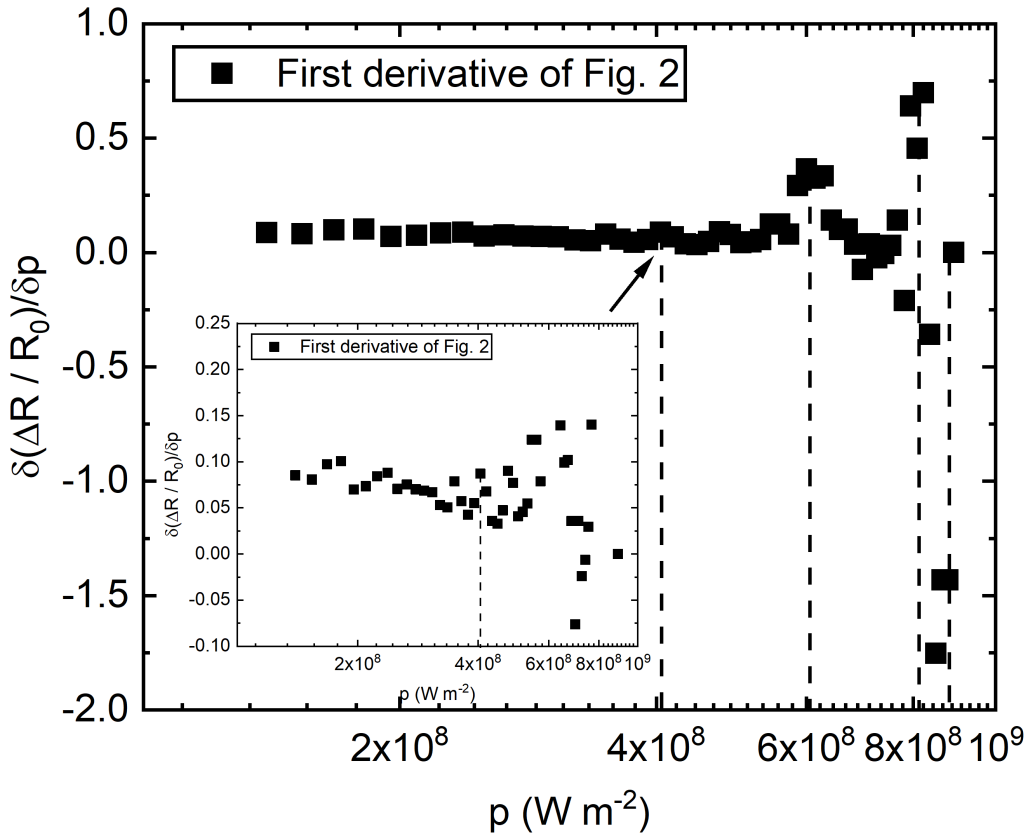
Figure S2. First derivative of our thermoreflectance data shown in Fig. 2 in the main manuscript. The inset shows the critical point near the power density of 4×10^8 W m^{-2} for clarity.

References

1.   J. L. Braun, D. H. Olson, J. T. Gaskins and P. E. Hopkins, "A steady-state thermoreflectance method to measure thermal conductivity," *Review of Scientific Instruments* **90**, 024905 (2019).

2.   A. D. Rakić, "Algorithm for the determination of intrinsic optical constants of metal films: application to aluminum," *Applied Optics* **34**, 4755-4767 (1995).

3.   I. H. Malitson, "Interspecimen Comparison of the Refractive Index of Fused Silica*,†,"
       Journal of the Optical Society of America **55**, 1205-1209 (1965).

4.   G. Bilalbegović and E. Tosatti, "Incomplete melting of the Au(100) surface," *Physical
       Review B* **48**, 11240-11248 (1993).